Tribology International 214 (2026) 111145

Contents lists available at ScienceDirect

Tribology International

journal homepage: www.elsevier.com/locate/triboint

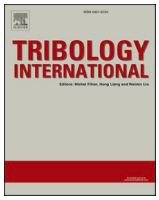

Full length article

Dynamic wettability of complex fractal isotropic surfaces – Multiscale correlations

Katarzyna Peta [a,*], Krzysztof J. Kubiak [b], Felice Sfravara [c], Christopher A. Brown [d]

[a] Institute of Mechanical Technology, Poznan University of Technology, Poznan 60-965, Poland
[b] School of Mechanical Engineering, University of Leeds, Leeds LS2 9JT, United Kingdom
[c] Department of Engineering, University of Messina, Contrada Di Dio (S. Agata), Messina 98166, Italy
[d] Mechanical and Materials Engineering Department, Worcester Polytechnic Institute, Worcester, MA 01609, USA

ARTICLE INFO

Keywords:
Lubrication
Wettability
Multiscale geometric analysis
Fractal theory
Surface complexity
Dynamic contact angle hysteresis

ABSTRACT

The complexity of surface topography can significantly influence the wettability, lubrication, and, in consequence, wear of materials in tribological contact. Therefore, wettability can be an important factor in contact lubrication. This research aims to find a correlation between a fractal, i.e., geometric, complexity of isotropic surfaces and the wettability at different observation scales. Surface wettability can be characterized under static and dynamic conditions by determining the dynamic contact angle hysteresis. Multiscale geometric correlations of topographic complexity and advancing, receding contact angle interactions are used to discover the best observation scales for strong correlation with dynamic surface lubrication. The analytical results confirmed that there is a certain range of scales in which the correlation coefficients between topographic complexity and dynamic wettability are strong ($r > 0.9$). This paper describes a novel characterization of surface-functionality interactions by dynamic lubrication of isotropic surfaces in a multiscale aspect.

1. Introduction

1.1. Objectives

This paper explains the lubrication of isotropic complex surfaces according to the assumptions of scale-sensitive fractal analyses (aka multiscale geometric analyses) [1]. Texturing techniques, including electro-discharge, can create complex geometric surface features. The identification of these microgeometries depends on the scale of consideration. The scale, or size, of topographic features affects their correlations with surface functionalities [2]. This assumption indicates that the same surface presented at different scales can correlate differently with the contact angle, a measure of wettability and lubrication.

This paper applies a novel approach to surface-functionality interactions by considering dynamic lubrication of isotropic surfaces in a multiscale context. Previous papers describe the application of multiscale geometric analyses to static surface wetting using sessile droplet technique on a stationary, non-rotatable surface [3–5]. This paper extends previous research to better represent the behavior of fluids on moving surfaces, more common in the real world. Therefore, it is important to test the correlation strengths between the geometric complexity and wettability determined not only by static, but also by advancing and receding contact angles on tilted surfaces, at different scales of observation. Identification of the best scales for observing dynamic wetting is a novel application of scale-sensitive fractal analyses.

1.2. Definitions

The definition of scale in surface metrology has two meanings. Firstly, it describes the relationship between the dimensions of a real object and its graphical representation. Secondly, it specifies a certain narrow band of wavelengths or spatial frequencies, whose narrowness is comparable to the measurement sensitivity [6]. Here, the scale is considered in this second context. Scale is essential in the observation of surface topography and surface-related phenomena. The visibility of the detail of surface topographic features and their functional characteristics depends on the scale of observation. Thus, there is a range of scales at which wetting [7], lubrication [8], and wear [9] phenomena are best observed to show the strongest correlations.

Surface metrology incorporates various concepts for describing surfaces, such as roughness, texture, topography, and microgeometry. These are often used interchangeably in the colloquial description of

* Corresponding author.
E-mail address: katarzyna.peta@put.poznan.pl (K. Peta).

https://doi.org/10.1016/j.triboint.2025.111145
Received 2 July 2025; Received in revised form 19 August 2025; Accepted 26 August 2025
Available online 27 August 2025

surface characteristics. However, technically, roughness refers to ISO 25178–2 [10] parameters calculated directly from topographic heights (z) distributed on a regular grid in x and y coordinates and filtered according to ISO 21920 [11]. Texture, in accordance with ASME B46.1 [12], includes roughness, waviness, and lay. While topography, additionally considers form. Describing fine-scale surface features is conveniently described as microgeometry.

Correlations between surface topographic characterization parameters [13] and topographically related behaviors [14] at various observation scales are part of scale-sensitive fractal analyses [1]. These analyses describe surface topography using fractal shapes characterized by self-similarity at different scales and scale invariance. Therefore, fractal shapes look the same regardless of magnification. The self-similarity of fractals makes it possible to divide them into copies of themselves, but of different sizes. Geometrically, fractals are irregular, and their circumferential lengths and areas change with the scale of observation. These assumptions of fractal analyses were first described by Mandelbrot [15]. The application of Mandelbrot's conclusions was developed by Brown et al. [1] in scale-sensitive analyses of fractal surfaces.

Multiscale geometric analyses describe surfaces with four basic parameters: relative area, area-scale fractal complexity, relative length, and length-scale fractal complexity. Relative area is defined by the ratio of the calculated surface area at a certain scale and the nominal surface area. Area-scale fractal complexity (Asfc) is equal to −1000 times the slope of the logarithmic plot of relative area versus scale. Analogous calculations are performed for relative length and length-scale fractal complexity, taking into account length dimensions instead of area dimensions. For surfaces with irregular topography, relative areas and lengths increase with decreasing scale [1,12]. The fractal dimension is used in descriptions of fractal geometry and is calculated as the difference of two and two times the slope [16]. Log-log plots of relative area or length to scale include the calculation of coefficients of determination R^2 to assess the consistency of the surface complexity at specific scales [17].

Most engineering surfaces, as well as those occurring in nature, can be described multifractally at various scales [18]. The topography of these surfaces can be characterized by irregularity and complexity [19]. These surfaces are particularly distinguishable at finer scales of observation, and their characterization by fractal shapes can be applied [20]. Therefore, surface topographies can present differently at different scales physically and functionally, while topographic measurements ranging from sampling distance to measurement size [21]. Reliable descriptions of surfaces with fractal shapes begin below the smooth-rough crossover (SRC). A smooth surface described with Euclidean geometries at coarser scales can become rough at finer scales, and more suitably for substitution using fractal shapes and dimensions (Fig. 1) [22].

Multiscale geometric analyses can complement the description of

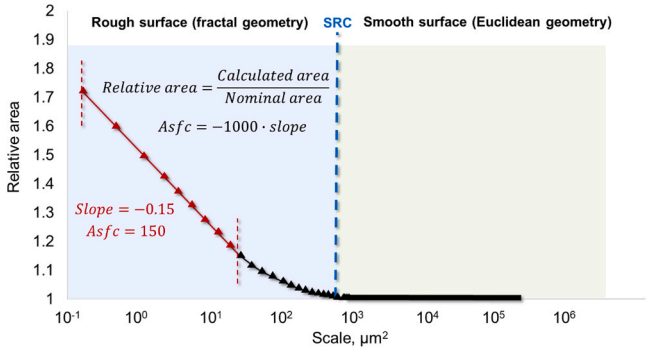

Fig. 1. Example log-log plot of relative area versus scale. Note: Relative areas greater than one define the smooth-rough crossover (SRC) and scales that discriminate smooth surfaces from rough ones.

topographically derived phenomena such as wetting and lubrication [3–5,7,8]. These phenomena underlie the interactions of atoms, ions and molecules, as well as forces at the interfaces of the liquid (liquid drop), solid (surface) and gas (air) phases [23]. The liquid on the surface is subject to three forces, called gravity, cohesion and capillary [24]. The description of wettability is based on Young's assumptions relating to the dependence of the contact angle and the energy state of the phase boundaries [25]. In practice, the contact angle is considered in a three-phase system and is determined geometrically by the angle between the tangents of the liquid drop and the solid surface. Young presented a simplified and basic model of wetting ideally smooth surfaces. Wenzel extended the wettability model with the r coefficient relating to the surface roughness [26], while Cassie-Baxter included surface fractions of different roughness [27].

Surface wettability can be considered in static and dynamic terms. The first one describes the contact angles of a sessile droplet on a surface under stable, non-moving three-phase boundaries [28]. The second one is associated with the movement of a droplet deposited on the surface. Here, wetting advancing angle and the de-wetting receding angle are recognized [29]. A valuable perspective on surface wettability is contact angle hysteresis, which involves subjecting a three-phase contact line to an external force [30]. A common method for measuring dynamic contact angle hysteresis is to observe the advancing and receding contact angles on a tilted solid surface [31], in contrast to static contact angle hysteresis, which is associated with the spreading of a liquid on a non-rotatable solid surface [32].

The interactions at the three-phase liquid-solid-vapor interface are governed by the wetting models described by the Young, Wenzel, and Cassie-Baxter equations [33]. Although these models strictly refer to static contact angles, certain assumptions can also be applied to dynamic contact angles of drops on tilted surfaces (Fig. 2) [34]. Young's ideal theory assumes smooth surfaces, and liquids not subject to external forces. The contact angle θ is the resultant of the equilibrium of surface tensions between the phases: solid-vapor (γ_{SV}), solid-liquid (γ_{SL}), and liquid-vapor (γ_{LV}) [35]. However, the modification of Young's equation for the contact angle hysteresis purposes is a mathematically simple procedure introducing the advancing θ_A and receding θ_R contact angles, as described theoretically by Tadmor [36] and practically verified by Chibowski et al. [37]. In reality, surfaces are rough in the nano, micro or macro range. Therefore the roughness coefficient is important in wetting studies. In the Wenzel model [26], the r coefficient is related to the surface topographic parameter Sdr [13], and the liquid droplet is in topographic valleys, typically for hydrophilic surfaces [38]. In the Cassie-Baxter model [27], the fractions of the surface area in contact with the liquid are considered, and the droplet is embedded on topographic peaks, characteristically of hydrophobic surfaces [39]. The way the drop is deposited on the surface causes the contact angle hysteresis to be higher in the Wenzel model and lower in the Cassie-Baxter model [40]. McHale et al. [41] colloquially described liquid-surface interactions as "sticky" in the Wenzel model and "slippy" in the Cassie-Baxter model. The particular structure of the surface microgeometry and the properties of the liquid can cause the occurrence of metastable states. A drop deposited on topographic peaks described by the Cassie-Baxter model can, under the influence of external forces and time, fill topographic valleys in accordance with the Wenzel model [42,43].

1.3. Rationale

Most surfaces found in nature can be described by self-similar fractal shapes [1]. The detail of the surface presentation depends on the size of the tiles constituting the surface. This is important for facilitating the description of rough surfaces with irregular geometric features. Surfaces are usually too irregular for classical geometric description [44]. Therefore, fractal description addresses these difficulties and simplifies correlations with surface-derived properties, such as wettability and

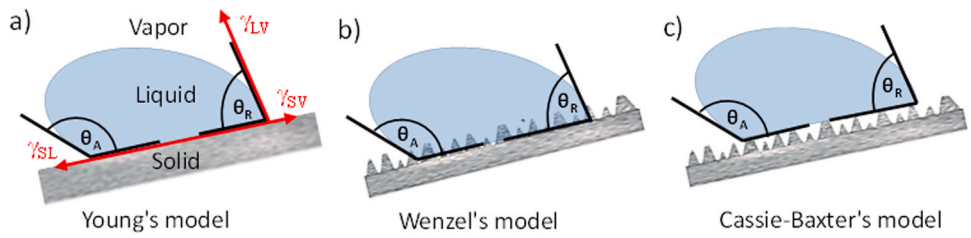

Fig. 2. Typical graphical interpretations of wetting of tilted surfaces related to: a) Young's model, b) Wenzel's model, c) Cassie-Baxter's model.

lubrication, at various scales of observation [45]. Surface representation with fractal shapes can be useful in understanding the dynamic behavior of liquids on surfaces. Scale-sensitive fractal analyses calculate the correlation coefficient between the surface fractal complexity and the dynamic contact angles at different scales. This allows identification of the best range of scales for the interaction between surface microgeometries and wettability. Multiscale correlations of complex fractal surfaces and wettability are important in the design and improvement of processes and products, as well as quality control. Analysis of surface-derived phenomena can require different representations of the same surface and knowledge of the interaction scales. Therefore, scales are essential to understanding phenomena occurring on surfaces.

1.4. State-of-the-art

In recent years, there has been a significant development in the use of scale-sensitive fractal analyses in relation to surface functionalities. Important contribution in area-scale and length-scale correlations and discriminations of functional surfaces were carried out by Brown [1,46], continuing Mandelbrot's work on the description of surfaces using fractal dimensions [15]. Brown et al. applied scale sensitive fractal analyses to determine: 1) adhesion strengths of surfaces created by abrasive blasting and thermal spray coating [17], 2) discrimination of rough surfaces obtained by turning at different feeds per revolution [47], 3) the interaction of surface roughness and tribological phenomena [48], mainly regarding 4) friction studies [3,49]. Stemp et al. adopted scale-sensitive fractal analyses to discriminate archaeological surfaces with and without microwear [50–52], while Peta et al. distinguished fingerprints [53]. Calandra et al. correlated tooth microtextures with the proportion and type of food consumed [54]. An unconventional application of scale-sensitive fractal analyzes was described by Cantor et al. [55], who examined cracked chocolate surfaces as a result of three-point bending at various temperatures.

Scale-sensitive fractal analyses can also discriminate the wettability and lubrication of textured surfaces. Peta et al. analyzed wettability of surfaces after electro-discharge machining [4,7,8]. The studies indicate the range of scales in which the correlations of wetting and surface fractal complexity are the highest. These authors' works have so far focused on the static contact angle. Bartkowiak et al. analyzed the wettability of surfaces created by three additive manufacturing methods and then correlated the built-up angle with the static contact angle at different scales [5]. Brown presented static contact angle results on a ground ski base [3]. These studies apply the scale-sensitive fractal analyses in sport surfaces.

Wettability and lubricity of surfaces are mostly described by the static contact angle as a basic measure. However, the dynamics of liquids on surfaces are also valuable, especially in understanding the behavior of liquids on moving surfaces, which often occurs in nature [56–58]. Wu et al. modeled contact angle hysteresis based on the fractal structure of contact line [59]. This study focused on determining the equilibrium contact angle for static contact angle hysteresis measurements. Although, Mortazavi et al. concluded that the fractal dimension is not sufficient to infer the strong correlation with the contact angle hysteresis and more thorough fractal analyses of surfaces are required [60].

1.5. Approach

Scale-sensitive fractal analyses for contact angle hysteresis have not yet appeared in the literature. Fractal shapes representing the surface can correlate with dynamic wettability, similarly to the static wettability described by the authors in previous works [4,7,8]. Therefore, the novelty of this study focuses on the multiscale correlations of surface complexity and advancing/receding contact angles, related to the dynamic contact angle hysteresis. So far, the published literature describes scale-sensitive fractal analyses only for static contact angles on rough surfaces. This paper aims to identify the best ranges of scales for observing dynamic wetting phenomena on isotropic surfaces, which commonly occur in engineering applications. Schematic representation of the research approach is provided in Fig. 3.

2. Material and methods

The surface microtextures of the grade 5 titanium alloy were obtained by electrical discharge machining and measured with a Bruker Alicona InfiniteFocus G5 focus variation 3D microscope. Topographic measurements were performed at 20x magnification, vertical resolution 0.05 μm, lateral resolution 1.32 μm and lateral sampling distance 0.44 μm. MountainsMap 9 software from DigitalSurf was used to preprocess the topographic measurement data set, as least squares surface leveling, material ratio-based thresholding, outlier removal, and filling in non-measured points. Then, conventional (ISO 25718–2) [13] and multi-scale geometric (ASME B46.1 appendix K) [12] surface characterization parameters were calculated. Conventional roughness parameters were calculated for the primary extracted surfaces after cutting off the shortest wavelengths, mostly related to measurement noise, with an S-filter. Gaussian filtering with a nesting index of 0.25 mm was used.

The surface wettability was determined from the dynamic contact angle hysteresis, measured on an optical goniometer with table tilt adjustable from 0° to 90°. The camera recorded the contact angles between the wetted surface and the tangent to the drop at a speed of 1 frame per 0.2 s. The recording of droplet images started from the 0° surface position, then the tilt was changed by 15° every 2 s, up to 90°. Measurements of the dynamic contact angle hysteresis allowed the determination of the static, advancing and receding contact angles by using droplet shape fitting according to the Young-Laplace equation. Wettability was tested with deionized water with a drop volume of 7 μl. The procedure for measuring the dynamic contact angle hysteresis at several table tilts is shown in Fig. 4.

Surface topographies and wettability were measured in 5 random positions for each surface of different complexity. The results are the arithmetic means of these measurements. First, surfaces were ultrasonically cleaned for 3 min in distilled water, rinsed with isopropyl alcohol and then acetone. For all measurements, stable and comparable ambient conditions were ensured, including temperature of 23° C and relative humidity of 45 %.

Scale-sensitive fractal analyses were used to correlate the topographic complexity with static, advancing, receding contact angles and contact angle hysteresis over a range of observation scales (from 0.58 μm^2 to 1318,420 μm^2). Area-scale calculations are adequate for isotropic

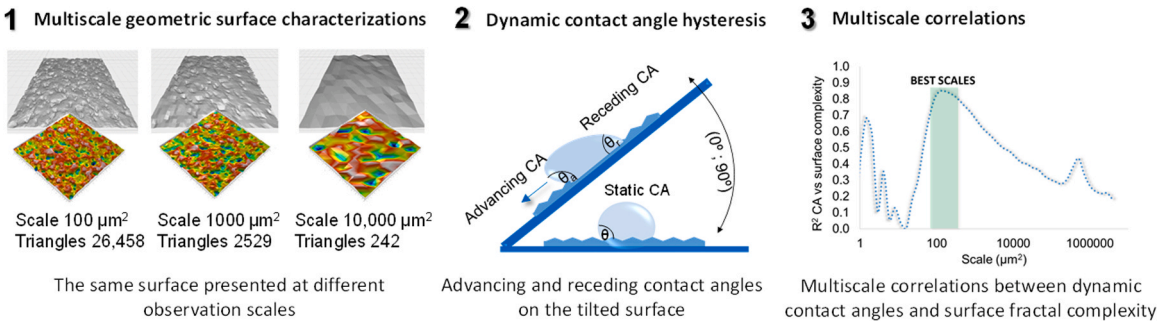

Fig. 3. Scheme of the research approach.

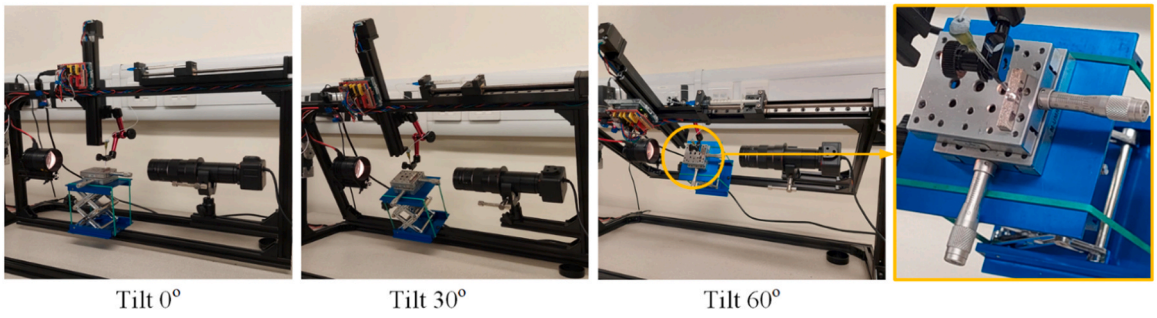

Fig. 4. Schematic view of the dynamic contact angle hysteresis measurements.

surfaces. Accordingly, area-scale fractal complexities (Asfc) and relative areas (RelA) were analyzed. The strength of relationships between Asfc and drop behavior related to dynamic contact angle hysteresis were determined by the coefficients of correlation, r, at all the scales. The correlations between these dependencies were determined by the Pearson correlation coefficient (r), indicating the relations of standard deviations from the means of both variables. In multiscale geometric analyses, the scales of occurrence of the strongest linear correlations of both variables were identified, both positive and negative, adequately therefore close to + 1 and - 1. Accordingly, increasing topographic complexity can lead to a trend of increasing wettability ($r > 0$) or decreasing wettability ($r < 0$). A correlation coefficient equal to 0 indicated no linear correlation between variables.

3. Results and discussion

Typical 3D images of textured isotropic surfaces are shown in Fig. 5. Focus variation microscopy adjusts the sharpness of the image at different focal positions in the z-axis of the optical system. This microscopy method is reliable for measurements of the rough and cratered surfaces considered in these studies [61]. Each surface can be characterized by conventional height and hybrid topographic parameters (Sa, Sq, Ssk, Sku, Sp, Sv, Sz, Sdq, Sdr) and their fractal dimensions (Das).

Significant, additional information about textured surfaces is provided by multiscale geometric parameters. Relative area (Fig. 6a) and area-scale complexity (Fig. 6b) characterize and discriminate surfaces at different observation scales. Relative areas were calculated by the patchwork method, in which the surfaces were fit multiple times with different sized triangular tiles whose areas area define the scale. Therefore, at each scale the relative area refers to the ratio of the calculated area to the nominal area. Area-scale complexity is a finite scale-based derivative of relative areas, which relates to the slopes on logarithmic plots of relative areas versus scales.

Isotropic surfaces have applications in tribological systems, particularly for trapping lubricant in surface irregularities regardless of the surface's rotational or sliding motion. A particular example of statistically isotropic surfaces in terms of crater and peak distribution are electrical discharge machined surfaces. The size of the craters can influence both lubricant retention and the effects of droplet pinning and sliding during dynamic motion. The isotropic distribution of the cavities results in uniform lubrication in all directions. In practice, electrical discharge machining is used for difficult-to-machine materials, including titanium alloys. The texture obtained by this process can shape medical implants in terms of osseointegration and wettability with body fluids, or efficiently distribute lubricating oil in aircraft engine systems. Gao et al. noticed that anisotropic roughness affects the contact angle hysteresis and friction by changing the droplet spreading kinetics [62]. These important conclusions were revised in this study in the context of isotropic surfaces.

Dynamic contact angle hysteresis reflects the behavior of liquids on tilted surfaces, common in real-world conditions. This can be significant in boundary lubrication by influencing the friction coefficient, and consequently, the wear rate of materials in tribological contact. Lubricants on inclined surfaces flow easily on smoother topographies and with low contact angle hysteresis, while lubricant retention in surface valleys occurs at higher contact angle hysteresis. Dynamic contact angle hysteresis can be determined by surface texturing. Here, isotropic textures are characterized by similar lubricant flow in all topographic directions. The size of the surface craters formed affects lubricant retention during surface inclination.

Droplet behavior on tilted surfaces is related to wetting models. Hydrophobic and superhydrophobic surfaces are most often described by the Cassie-Baxter wetting model with possible Wenzel metastable states, while the droplet on the tilted surface rolls or slides with low contact angle hysteresis. Here, the surfaces were textured into hydrophilic and nearly hydrophobic characterized by the Wenzel model. A friction-slip movement of the droplets was observed with significant contact angle hysteresis depending on the surface complexity, limiting the smooth sliding of the fluid. In this model, the contact line of the droplet edge and the tilted surface is important. Initially, surface complexities pin the droplet. However, external forces of gravity and adhesion cause the building of an advancing angle, which, at a critical stage, causes the droplet and the contact line to shift. The movement of the droplet is uneven, with stops and crossings of barriers on surface

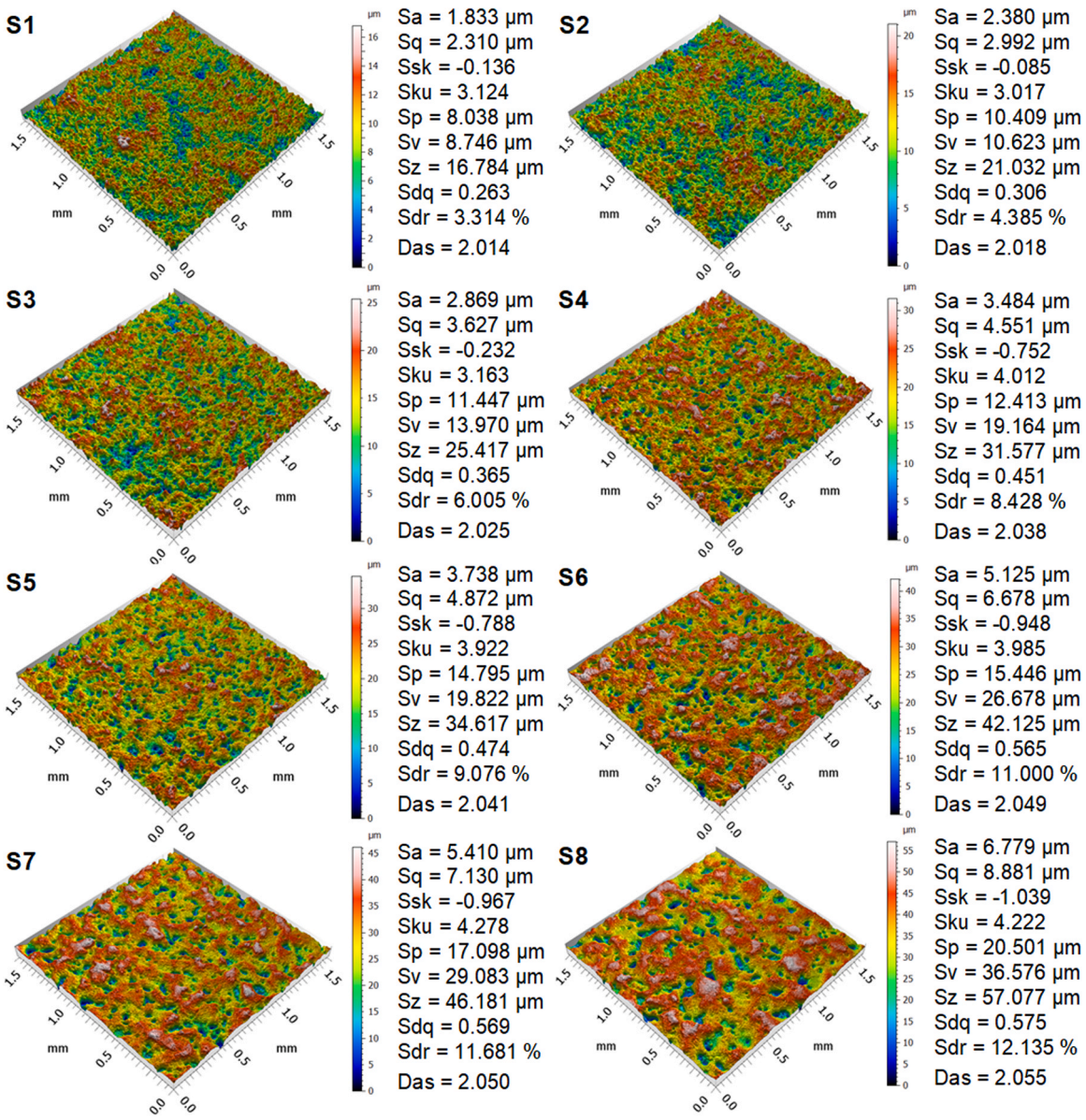

Fig. 5. Typical 3D images of textured surfaces along with conventional height and hybrid topographic parameters and fractal dimensions.

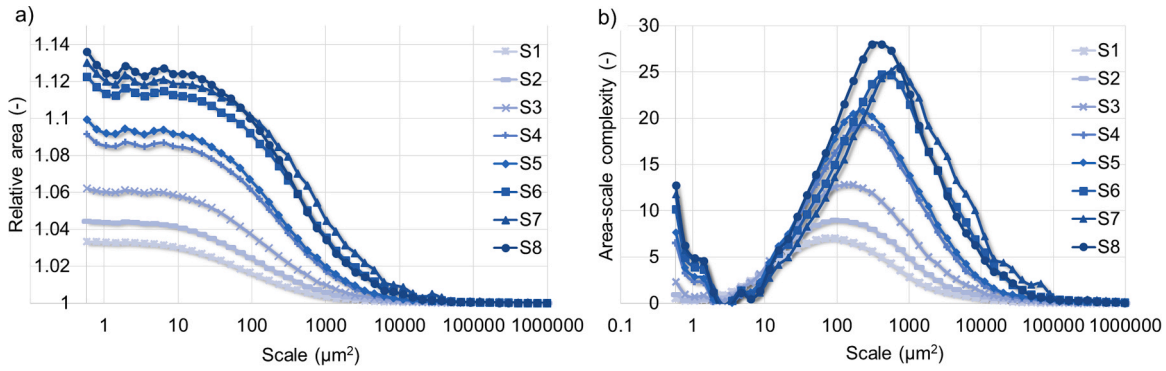

Fig. 6. Multiscale parameters describing textured surfaces: a) relative area, b) area-scale complexity. Note: Surfaces S1 to S8 are presented according to increasing roughness Sa, respectively.

irregularities.

In the hydrophilic range, increasing roughness causes greater droplet pinning to the surface and greater contact angle hysteresis associated with droplet motion. In previous works, the authors analyzed factors influencing surface wettability. Texture has been identified as the most important determinant of fluid behavior on surfaces. Although, apart

from topographic aspects, wettability is related to surface energy. Fluids spread more easily on a surface with higher surface free energy [8]. Moreover, for the functional dependencies of surface wetting, the characteristics directly related to the liquid drop are important. The viscosity of the liquid can significantly change the observed surface wetting [4]. Higher liquid viscosity results in lower hysteresis of the dynamic contact angle. Contact angles of droplet sizes that are too small or too large can be influenced differently by gravitational or capillary forces, confusing the surface influences [7]. In addition, the experiments are sensitive to vibrations, air flow, temperature and humidity changes [61]. Therefore, the comparability of the research results is most reliable when the same wetting liquid and conditions were applied. Additionally, one of the parameters influencing dynamic wettability is the rotational speed of the surface with the embedded droplet. Mohsen et al. observed that increasing the rotational speed of the surface reduces the droplet spreading time [63]. Lee et al. analyzed the effect of surface rotation speed on the maximum spreading velocity for three liquids of different viscosities. The studies showed that lower viscosity liquids spread more effectively for each analyzed surface rotation speed in the range of 0.2–4 m/s [64].

Dynamic contact angle hysteresis provides knowledge about the behavior of fluid on surfaces. Firstly, about the static contact angle of the droplet after deposition on the surface, secondly, about the advancing and receding contact angles during surface inclination, thirdly, about the sliding angle, and fourthly, about the dynamics of the droplet motion. Here, with the increase of surface topographic complexity, the advancing contact angle increases and the receding contact angle decreases, which consequently increases the contact angle hysteresis. The increase of surface inclination enhances the contact angle hysteresis. High contact angle hysteresis is synonymous with droplet pinning to topographic irregularities and intermittent droplet movement down the inclination. In contrast, low contact angle hysteresis is associated with smoother textures and greater droplet mobility.

Dynamic contact angle hysteresis describes both static and dynamic surface wetting (Fig. 7). The first points of the curve are determined by the static contact angle. The subsequent course of the curve is characterized by dynamic contact angle forced by tilting the surface with the deposited liquid drop.

The dynamic contact angle hysteresis is defined by the difference between the advancing and receding contact angles, and depends on the topographic characterization parameters (Fig. 8).

Static and dynamic wettability are dependent on the surface texture. Here, isotropic textures were discriminated by topographic characterization parameters [13], also called roughness parameters. Almost all parameters from the height and hybrid groups (Sa, Sq, Sp, Sv, Sz, Sdq, Sdr), related to the topographic heights but also steepness and texture complexity, showed a clear relationship with contact angle hysteresis ($r > 0.9$). In Wenzel's model, higher values of these roughness

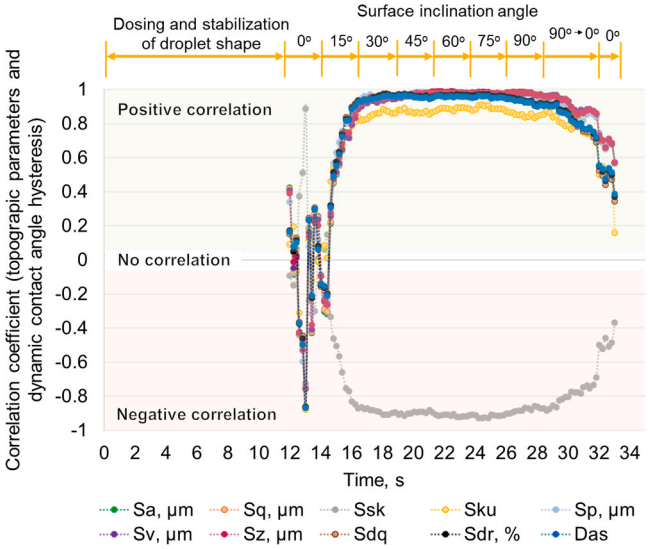

Fig. 8. Correlation coefficients between topographic characterization parameters and dynamic contact angle hysteresis.

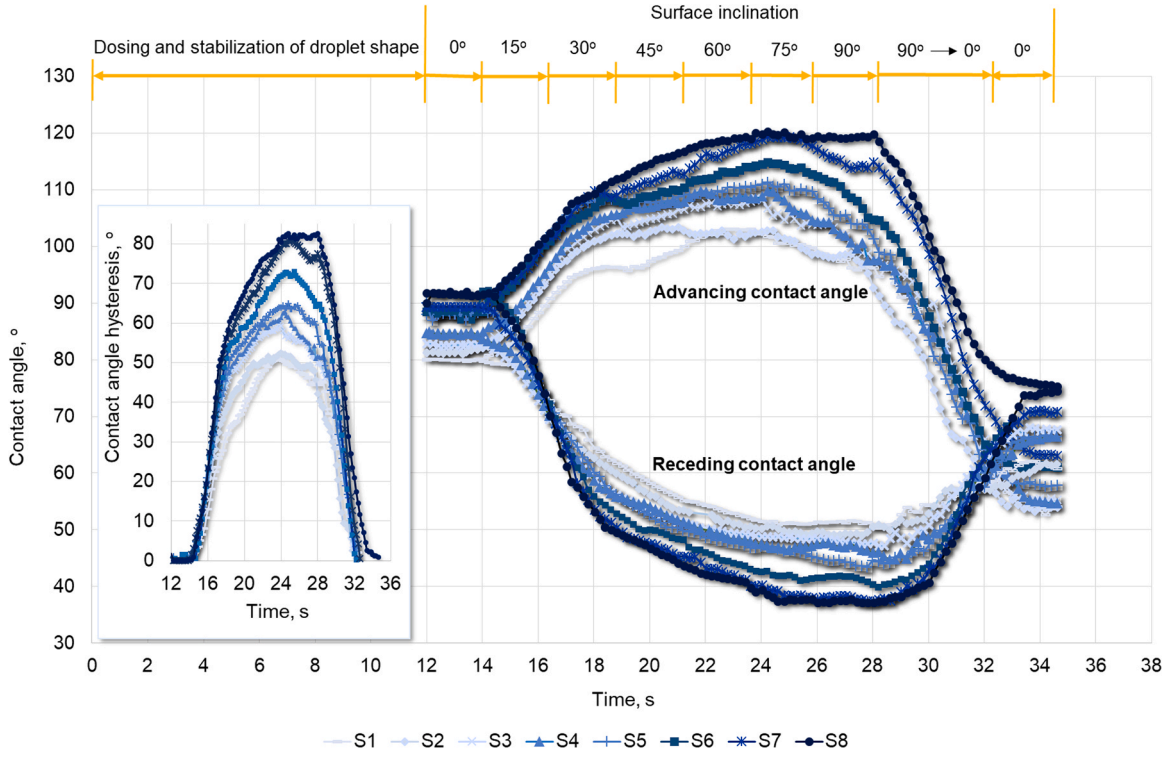

Fig. 7. Dynamic contact angle hysteresis for tilted surfaces S1-S8.

parameters reduce wettability and constitute the surface towards hydrophobicity. A similarly strong correlation with the dynamic contact angle hysteresis is noted for the surface fractal dimension. This indicates the fractal nature of the studied surfaces and the ability for their multiscale geometric characterizations. Slightly worse correlation coefficients ($-0.8 > r > 0.8$) were noted for Ssk and Sku. Therefore, skewness and kurtosis appear to be of limited effectiveness in capturing functional relationships. The only topographic parameter with negative correlation with the dynamic contact angle hysteresis is Ssk. Therefore, with increasing skewness, the dynamic contact angle hysteresis decreases. With the increase of all other topographic parameters (Sa, Sq, Sp, Sv, Sz, Sdq, Sdr, Sku), the dynamic contact angle hysteresis also shows an increasing trend. The ISO height parameters Sa, Sq (arithmetical mean and root mean square heights) describe the overall level of topographic heights, while the parameters Ssk, Sku (skewness and kurtosis) are sensitive to the shape of the topographic height distribution and the non-Gaussian roughness of the surface [62]. In these studies, negative skewness reduces the effective contact area and surface wettability. In shear flow, kurtosis can increase the lubricant film thickness and contact area, as determined by Gao et al. [62]. Ssk and Sku are based on global height distribution statistics and may not fully reflect local features important for surface wetting. The correlation of the surface topographic characterization parameters, fractal dimension, with the dynamic contact angle hysteresis is stable on the target surface inclinations. Coefficients of correlation, r, close to 0 were obtained for two stages of the dynamic contact angle hysteresis, the initial start of the surface tilt and for the final surface tilt from 90° to 0°. The initiation of an external force on the droplet caused it to tilt and take a relatively large jump in the surface tilt at 90° resulted in temporarily unstable contact angles. In all other stages of dynamic wettability, the correlation coefficients are at a comparable level, indicating a strong relationship between most of the surface topographic characterization parameters and the dynamic contact angle hysteresis.

Visualizations of typical droplet shapes on tilted surfaces with different textures are shown in Fig. 9. Surface texturing can change wettability. Here, textures are characterized by a static contact angle of 79.9° to 91.5°, which corresponds to the hydrophilic and para-hydrophobic characteristics. Tilting the surface changes the shape of the droplets relative to the texture. On smoother surfaces, the drops are characterized by a more flattened shape. Greater topographic barriers cause a greater increase in the advancing contact angle needed for droplet movement, for S8 surface up to 120°. In addition, the liquid droplet is more strongly attached to larger surface irregularities and moves with more difficulty. Droplets forced to move under the surface tilt, after returning to position 0°, are characterized by a divergence in the left and right contact angles, which results from the partial spreading of the droplet on the surface.

Multiscale geometric analyses are considered better than classical correlations of topographic characterization parameters and phenomena occurring on the surfaces. This results not only correlate topographic complexities with surface functional properties, but they also can indicate the best scales of observation in a wide range of considerations, from sampling distance to field of view. Multiscale analyses were used in this study for the first time to correlate topographic complexity with advancing contact angle, receding contact angle and dynamic contact angle hysteresis changing with time and with respect to surface inclination.

Multiscale geometric analyses identify relationships between surface

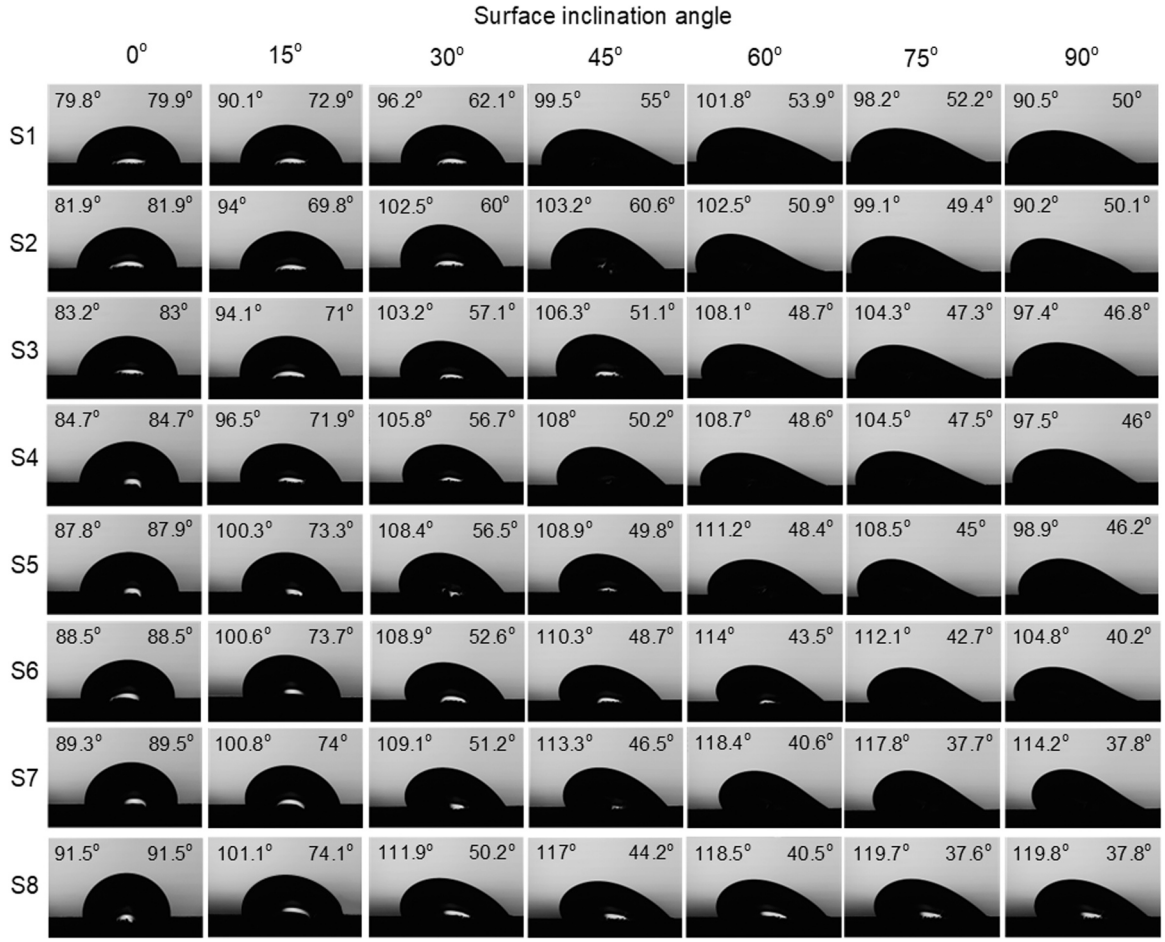

Fig. 9. Typical drop shapes on inclined surfaces S1-S8 with advancing and receding contact angles.

complexities and functional phenomena over a wide range of observation scales. Here, the assumptions of multiscale fractal theory are applied to characterize contact lubrication of complex isotropic surfaces. The strength of the relationships between surface complexity and dynamic wettability is assessed using the coefficients of correlation (r) over a range of scales from 0.58 μm^2 to 1318,420 μm^2. These relationships are visualized in 3D plots of the relationship between the coefficient of correlation, r, of the contact angle and the surface complexity (z-axis) versus the scale of observation (y-axis) as a function of time related to the dynamic wettability procedure and the surface inclination angle (x-axis). Additional 2D plots show the correlation coefficient (r) of topographic complexity (Asfc) and contact angles versus scale, at different

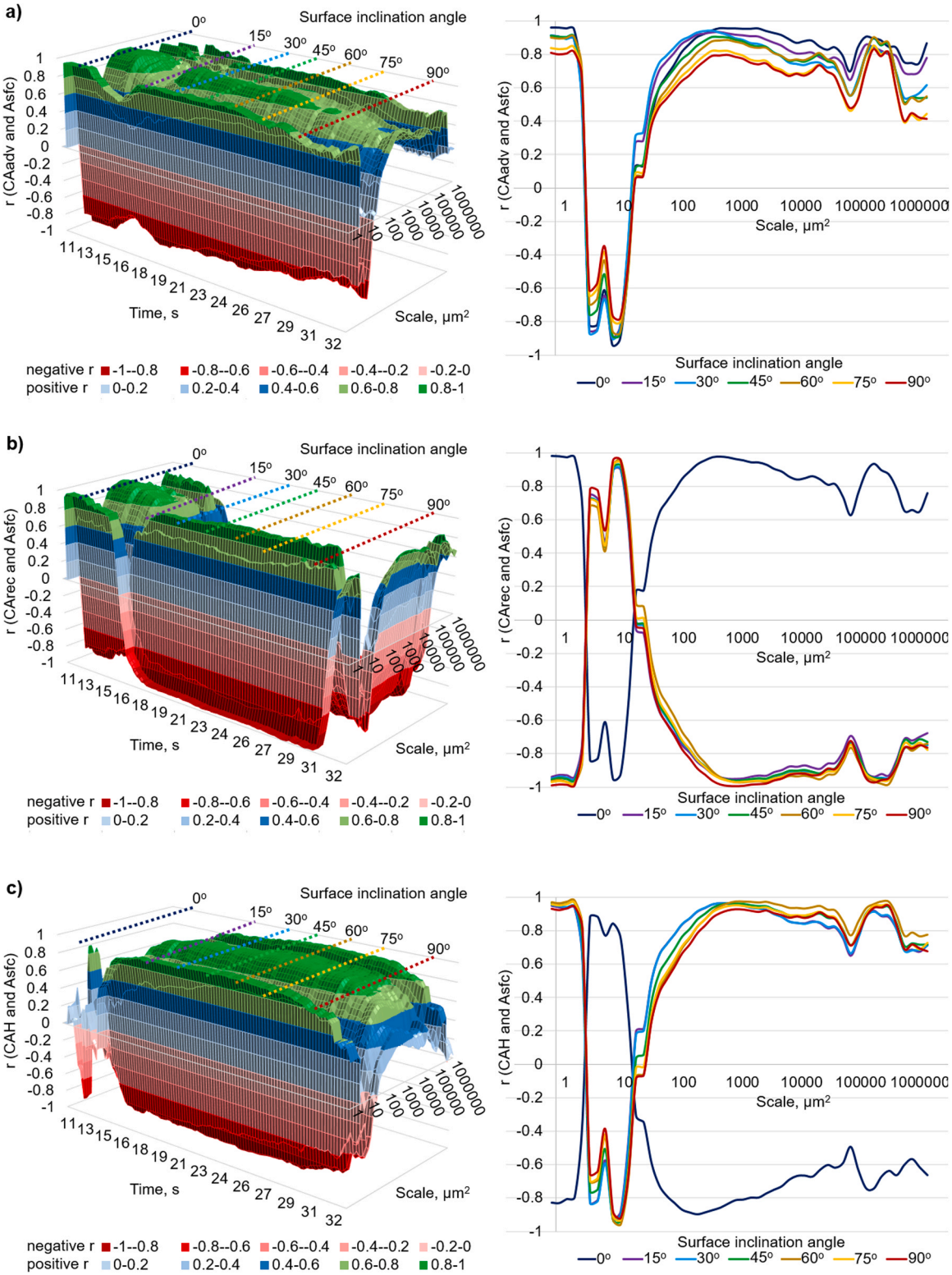

Fig. 10. Coefficients of correlation (r) at various observation scales, between surface complexity (Asfc) and: a) advancing contact angle (CAadv), b) receding contact angle (CArec), c) dynamic contact angle hysteresis (CAH).

surface inclinations. In these relationships, three important types of contact angles in dynamic wetting were considered: advancing contact angle, CAadv, (Fig. 10a), receding contact angle, CArec, (Fig. 10b), dynamic contact angle hysteresis, CAH, (Fig. 10c).

Surface topographic characterization parameters (Sa, Sq, Sp, Sv, Sz, Ssk, Sku, Sdq, Sdr) all showed a good correlation with dynamic wettability. However, multiscale geometric analyses additionally indicate the scales at which these correlations are strongest, and scales at which the occurrence of these correlations cannot be clearly indicated. In multiscale geometric analyses, surfaces are characterized by the area-scale fractal complexity (Asfc), correlated with surface functional parameters, in this case dynamic wetting. Surface complexity refers to the parameter area-scale fractal complexity (Asfc), following the nomenclature of scale-sensitive fractal analyses (aka multiscale geometric analyses) [1]. Asfc is equal to −1000 times the slope of the logarithmic plot of relative area versus scale. While, relative area describes the ratio of the area calculated at a given scale to the nominal surface area. Surface complexity is closely related to the smooth-rough crossover (Fig. 1). A smooth surface with Euclidean geometry at larger scales can become rough and complex at smaller scales, and can be described by fractals.

Three scale ranges show strong coefficients of correlation $r > 0.8$ or $r < -0.8$ between the dynamic wetting parameters and topographic complexity in all surface inclinations (15°-90°). The given scale ranges are universal for all dynamic wetting parameters (advancing contact angle, receding contact angle, contact angle hysteresis): 0.58 μm^2 - 1.43 μm^2, 309 μm^2 - 756 μm^2, 163,107 μm^2 - 219,851 μm^2. In the range of the smallest and largest scales, small surface inclinations up to 30° and the largest from 75° correlate about 10 % worse. Advancing contact angles correlate weaker with surface complexity at higher surface inclinations. This is due to the motion of the droplet, which slightly changes shape and contact angle during flow. Receding contact angle overcomes topographic barriers to a lesser extent and changes values more smoothly when increasing the surface inclination. Dynamic contact angle hysteresis is the result of trends from both contact angles, advancing and receding ones. Therefore, at higher surface inclinations, a slight decrease in the correlation of topographic complexity and dynamic contact angle hysteresis is noted.

The dynamic surface wetting experiment indicates the starting point of droplet motion on the surface. This motion is associated with specific contact angles and surface inclinations that can correlate strongly with the surface complexities. Fig. 11a shows the sliding angle, advancing contact angle, receding contact angle and contact angle hysteresis causing the motion of the droplet on the surface. Fig. 11b presents the coefficients of correlation (r) of surface complexity and sliding / advancing / receding / hysteresis contact angles at the time of droplet motion with respect to different observation scales.

The critical point of the dynamic contact angle hysteresis is the start of the droplet movement on the surface along the contact line. This point is characterized by the maximum advancing contact angle built on the topographic barrier just before flow, as well as the sliding angle identifying the surface inclination angle causing the droplet movement. The topographic complexity of the surface is directly proportional to the sliding angle, advancing angle and dynamic contact angle hysteresis, and inversely proportional to the receding contact angle. The initiation of droplet motion is best observed on the scales 309 μm^2 −756 μm^2, for which the surface complexity and dynamic wetting parameters correlate with the coefficient of correlation $r > 0.9$ for advancing contact angle, contact angle hysteresis, sliding angle, and $r < -0.9$ for receding contact angle.

Multiscale geometric analysis enhances the characterization of surface topography and surface phenomena. Tiling the surface with different sizes of triangles, within the sampling distance and field of view of the measuring instrument, presents a surface with different levels of topographic complexity. Analysis of the dynamic behavior of liquids on such tiled surfaces is important in modeling and understanding the dynamic aspects of wettability and lubrication. Thus, at the finest scales, it is assessed how the finest microgeometric features, surface microroughness, affect the dynamic contact angle hysteresis and the contact line shift of the liquid droplet and the solid surface. At coarser scales, it is indicated how larger topographic features, e.g. craters, affect dynamic wettability. Multiscale geometric analysis, including both fine and coarse scales, identifies which surface topographic complexity most strongly correlates with wetting and lubrication.

The observed correlations between conventional ISO and multiscale topographic surface parameters and dynamic contact angle hysteresis result from topographic barriers affecting the contact line. Although, surface energy heterogeneity, described in more detail in the authors' earlier work [8], also contributes significantly to the dynamic wetting of complex surfaces. In practice, the identification of functional correlations depends on characterizing the topography at different scales with respect to geometric accuracy. Macroscopic phenomena, including dynamic wettability, can be viewed as the sum of discrete interactions occurring at fine scales along the liquid-solid contact line. As a result, the contact line is irregular due to the surface irregularity. Dynamic contact angle hysteresis, which captures the sequence of contact angles, varies as a result of local inclinations of the surface tiles. The surfaces were characterized using triangular tiles, which forms the basis of scale-sensitive fractal analysis. At fine scales, these differences in tiles inclinations may not be sufficiently visible and may suggest the droplet to behave as on a smooth surface. A correspondingly larger tiles inclination at certain scales affects the contact angles and overcomes the smoothing of liquid droplets by surface tension. At coarser scales, larger variations in tile inclinations can pin the contact line more effectively,

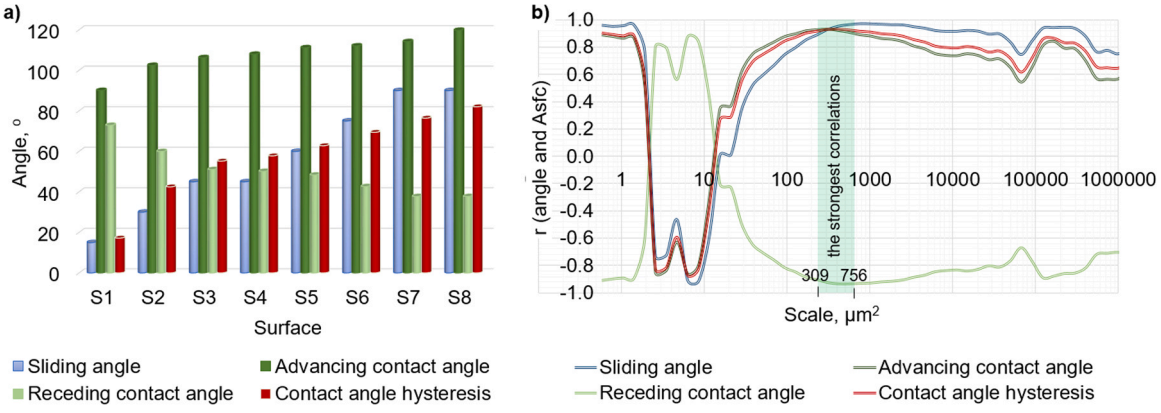

Fig. 11. Dynamic wettability parameters starting the droplet movement on the tilted surface: a) sliding, advancing, receding contact angles, and dynamic contact angle hysteresis, b) coefficient of correlation, r, between dynamic wettability parameters and surface complexity (Asfc) versus observation scale.

thus influencing dynamic contact hysteresis. Similar conclusions were presented by Brown et al., who studied the behavior of liquids on the ski surface [3].

This work focuses on empirical multiscale correlations between surface fractal complexity and dynamic contact angle hysteresis. However, these scale-dependent correlations can provide the basis for contact models describing lubricant entrapment and boundary film stability. Gao et al. demonstrated that surface isotropy/anisotropy and non-Gaussian roughness are important for contact pressure distribution and lubricant film formation in mixed lubrication [62,65]. The findings of Gao et al. in these two significant studies suggest that the established contact models, extended with multiscale characteristics of dynamic surface wettability, can more thoroughly explain lubricant film durability, droplet pinning, and contact line dynamics. The mixed lubrication contact model, based on both elastic–plastic and hydrodynamic theories, incorporates the effects of normal pressure, surface roughness, relative movement velocity, and lubricant viscosity to improve the mechanical interface between the solid and liquid contact parts. It can be concluded that the efficiency of mixed lubrication can be adjusted by surface roughness and the average gap between the contacting surfaces. However, minimizing surface asperities enables the transition to a fully lubricated contact regime. These findings highlight the scale-dependent character of surface topographic complexity and mixed lubrication. Multiscale analyses therefore reveal a scale of asperities that best correlates with lubrication in contact mechanics. These experimental studies can draw on theoretical algorithms that preserve constant physical aspects [66–69]. This provides a perspective for future simulation work that models dynamic contact angle hysteresis at various observational scales. Knowledge of the dynamic behavior of liquid drops on a tilted surface may lead to the development of predictive methods for contact angle evolution.

4. Conclusions

Surface textures of different topographic complexity correlate strongly with dynamic wettability and lubrication. These studies consider which surface topographic complexities correlate most strongly with dynamic contact angle hysteresis. The novelty of this study is the application of multiscale geometric characterizations identifying the best range of scales for observing dynamic phenomena coexisting with contact angle hysteresis during surface tilting with a deposited liquid droplet. Dynamic wettability more reliably reflects the real conditions of most engineering surfaces.

The most important conclusions from this study are that:

1. Multiscale geometric analyzes identify the best observation scales (from 309 μm^2 to 756 μm^2) at which dynamic contact angle hysteresis best correlates with topographic complexity.
2. Static and dynamic wettability depends on the surface topographic complexity.
3. Conventional (Sa, Sq, Sp, Sv, Sz, Sdq, Sdr) and multiscale (area-scale complexity) topographic characterization parameters correlate strongly with dynamic contact angle hysteresis ($r > 0.9$).
4. The topographic complexity of the surface, if it increases, reduces wettability.
5. Hydrophilic textured surfaces are consistent with the Wenzel model, in which droplets on rough, inclined surfaces perform friction-slip movement.
6. An increase in surface complexity intensifies droplet pinning at topographic irregularities, while also facilitating partial motion in the direction of surface inclination.
7. The significant point of the dynamic contact angle hysteresis is the start of the droplet movement on the surface along the contact line.
8. Dynamic wettability can be an important factor in contact lubrication.

Future studies are planned to continue multiscale correlations, demonstrating the relationship between anisotropic surfaces and dynamic contact angle hysteresis.

Statement of Originality

We confirm that this work is original and has not been published elsewhere, nor is it currently under consideration for publication elsewhere.

Dynamic wettability of complex fractal isotropic surfaces – multiscale correlations, authored by Katarzyna Peta, Krzysztof Kubiak, Felice Sfravara, and Christopher A. Brown.

CRediT authorship contribution statement

Katarzyna Peta: Writing – review & editing, Writing – original draft, Visualization, Validation, Supervision, Software, Resources, Project administration, Methodology, Investigation, Funding acquisition, Formal analysis, Data curation, Conceptualization. **Krzysztof J. Kubiak:** Writing – review & editing, Writing – original draft, Visualization, Validation, Supervision, Software, Resources, Methodology, Investigation, Formal analysis, Conceptualization. **Felice Sfravara:** Writing – review & editing, Writing – original draft, Formal analysis. **Christopher A. Brown:** Writing – review & editing, Writing – original draft, Software, Formal analysis.

Declaration of Competing Interest

The authors declare that they have no known competing financial interests or personal relationships that could have appeared to influence the work reported in this paper.

Acknowledgements

This research was funded by the National Science Centre, Poland, under the program MINIATURA 7, grant number 2023/07/X/ST8/01233.

Data availability

Data will be made available on request.

References

[1] Brown CA, Hansen HN, Jiang XJ, Blateyron F, Berglund J, Senin N, et al. Multiscale analyses and characterizations of surface topographies. CIRP Ann 2018;67:839–62. https://doi.org/10.1016/j.cirp.2018.06.001.
[2] Belaud V, Valette S, Stremsdoerfer G, Bigerelle M, Benayoun S. Wettability versus roughness: Multi-scales approach. Tribol Int 2015;82:343–9. https://doi.org/10.1016/j.triboint.2014.07.002.
[3] Brown CA. Surface metrology principles for snow and ice friction studies. Front Mech Eng 2021;7. https://doi.org/10.3389/fmech.2021.753906.
[4] Peta K, Bartkowiak T, Galek P, Mendak M. Contact angle analysis of surface topographies created by electric discharge machining. Tribol Int 2021:107139. https://doi.org/10.1016/j.triboint.2021.107139.
[5] Bartkowiak, Peta T, Królczyk K, Niesłony JB, Bogdan-Chudy P, Przeszłowski M, et al. Wetting properties of polymer additively manufactured surfaces – multiscale and multi-technique study into the surface-measurement-function interactions. Tribol Int 2025;202. https://doi.org/10.1016/j.triboint.2024.110394.
[6] Bartkowiak T, Brown CA. A characterization of Process-Surface texture interactions in Micro-Electrical discharge machining using multiscale curvature tensor analysis. J Manuf Sci Eng Trans ASME 2018;140. https://doi.org/10.1115/1.4037601.
[7] Peta K. Multiscale wettability of microtextured irregular surfaces. Mater (Basel) 2024;17:18. https://doi.org/10.3390/ma17235716.
[8] Peta K, Bartkowiak T, Rybicki M, Galek P, Mendak M, Wieczorowski M, et al. Scale-dependent wetting behavior of bioinspired lubricants on electrical discharge machined Ti6Al4V surfaces. Tribol Int 2024;194. https://doi.org/10.1016/j.triboint.2024.109562.
[9] Peta K, Stemp WJ, Chen R, Love G, Brown CA. Multiscale characterizations of topographic measurements on lithic materials and microwear using a GelSight max: investigating potential archaeological applications. J Archaeol Sci Rep 2024;57. https://doi.org/10.1016/j.jasrep.2024.104637.

[10] ISO 25178-2:2012. Geometrical Product Specifications (GPS)—Surface Texture: Areal—Part, 2. International Organization for Standardization. Geneva, Switzerland: 2012.
[11] ISO 21920-1:2021 Geometrical product specifications (GPS) — Surface texture: Profile. 2021.
[12] ASME B46.1. Surface texture: surface roughness, waviness, and lay. New York: American Society of Mechnical Engineers; 2019.
[13] 25178-2 DI. DS/EN ISO 25178-2. Geometrical product specification (GPS) - Surface texture: Areal - Part 2: Terms, definitions and surface texture parameters. Danish Stand Found 2012.
[14] Kubiak KJ, Wilson MCT, Mathia TG, Carval P. Wettability versus roughness of engineering surfaces. Wear 2011;271:523–8. https://doi.org/10.1016/j.wear.2010.03.029.
[15] Mandelbrot BB. The fractal geometry of nature. New York: WH freeman; 1982.
[16] Schuller DJ, Rao AR, Jeong GD. Fractal characteristics of dense stream networks. J Hydrol 2001;243:1–16. https://doi.org/10.1016/S0022-1694(00)00395-4.
[17] Brown CA, Siegmann S. Fundamental scales of adhesion and area-scale fractal analysis. Int J Mach Tools Manuf 2001;41:1927–33. https://doi.org/10.1016/S0890-6955(01)00057-8.
[18] Brown CA. Areal fractal methods. Character Area Surf Texture 2013;9783642364:129–53. https://doi.org/10.1007/978-3-642-36458-7_6.
[19] Macek W, Branco R, Podulka P, Masoudi Nejad R, Costa JD, Ferreira JAM, et al. The correlation of fractal dimension to fracture surface slope for fatigue crack initiation analysis under bending-torsion loading in high-strength steels. Meas J Int Meas Confed 2023;218. https://doi.org/10.1016/j.measurement.2023.113169.
[20] Stemp WJ, Lerner HJ, Kristant EH. Testing Area-Scale fractal complexity (Asfc) and laser scanning confocal microscopy (LSCM) to document and discriminate microwear on experimental quartzite scrapers. Archaeometry 2018;60:660–77. https://doi.org/10.1111/arcm.12335.
[21] Stemp WJ. A review of quantification of lithic use-wear using laser profilometry: a method based on metrology and fractal analysis. J Archaeol Sci 2014;48:15–25. https://doi.org/10.1016/j.jas.2013.04.027.
[22] Leach R. Characterisation of areal surface texture. Character Area Surf Texture 2024. https://doi.org/10.1007/978-3-031-59310-9.
[23] Mukherjee B, Chakrabarti B. Wetting behavior of a Three-Phase system in contact with a surface. Macromolecules 2022;55:3886–97. https://doi.org/10.1021/acs.macromol.1c02559.
[24] Wojciechowski L, Kubiak KJ, Mathia TG. Roughness and wettability of surfaces in boundary lubricated scuffing wear. Tribol Int 2016;93:593–601. https://doi.org/10.1016/j.triboint.2015.04.013.
[25] Young III T. An essay on the cohesion of fluids. Philos Trans R Soc Lond 1805;95:65–87. https://doi.org/10.1098/rstl.1805.0005.
[26] Wenzel RN. Resistance of solid surfaces to wetting by water. Ind Eng Chem 1936;28:988–94. https://doi.org/10.1021/ie50320a024.
[27] Cassie ABD, Baxter S. Wettability of porous surfaces. Trans Faraday Soc 1944;40:546–51. https://doi.org/10.1039/tf9444000546.
[28] Xiong B, Li J, He C, Tang X, Lv Z, Li X, et al. Effect of pore morphology and surface roughness on wettability of porous titania films. Mater Res Express 2020;7. https://doi.org/10.1088/2053-1591/abc770.
[29] Xiao Y, Zheng J, He Y, Wang L. Droplet and bubble wetting behaviors: the roles of surface wettability and roughness. Colloids Surf A Physicochem Eng Asp 2022;653. https://doi.org/10.1016/j.colsurfa.2022.130008.
[30] Kubiak KJ, Wilson MCT, Mathia TG, Carras S. Dynamics of contact line motion during the wetting of rough surfaces and correlation with topographical surface parameters. Scanning 2011;33:370–7. https://doi.org/10.1002/sca.20289.
[31] Yildirim Erbil H. Dependency of contact angles on three-phase contact line: a review. Colloids Interfaces 2021;5. https://doi.org/10.3390/colloids5010008.
[32] Butt HJ, Liu J, Koynov K, Straub B, Hinduja C, Roismann I, et al. Contact angle hysteresis. Curr Opin Colloid Interface Sci 2022;59. https://doi.org/10.1016/j.cocis.2022.101574.
[33] Legrand Q, Benayoun S, Valette S. Quantification and modeling of anisotropic wetting of textured surfaces. Appl Surf Sci 2023;611. https://doi.org/10.1016/j.apsusc.2022.155606.
[34] Choi W, Tuteja A, Mabry JM, Cohen RE, McKinley GH. A modified Cassie-Baxter relationship to explain contact angle hysteresis and anisotropy on non-wetting textured surfaces. J Colloid Interface Sci 2009;339:208–16. https://doi.org/10.1016/j.jcis.2009.07.027.
[35] Wang F, Nestler B. Wetting and Contact-Angle hysteresis: density asymmetry and van der waals force. Phys Rev Lett 2024;132. https://doi.org/10.1103/PhysRevLett.132.126202.
[36] Tadmor R. Line energy and the relation between advancing, receding, and young contact angles. Langmuir 2004;20:7659–64. https://doi.org/10.1021/la049410h.
[37] Chibowski E, Terpilowski K. Surface free energy of sulfur-Revisited. I. Yellow and Orange samples solidified against glass surface. J Colloid Interface Sci 2008;319:505–13. https://doi.org/10.1016/j.jcis.2007.10.059.
[38] Moraila CL, Montes Ruiz-Cabello FJ, Cabrerizo-Vílchez M, Rodríguez-Valverde MÁ. Wetting transitions on rough surfaces revealed with captive bubble experiments. The role of surface energy. J Colloid Interface Sci 2019;539:448–56. https://doi.org/10.1016/j.jcis.2018.12.084.
[39] Maghsoudi K, Momen G, Jafari R. The thermodynamic stability of the Cassie–Baxter regime determined by the geometric parameters of hierarchical superhydrophobic surfaces. Appl Mater Today 2023;34. https://doi.org/10.1016/j.apmt.2023.101893.
[40] Bush J.W.M. 15. Contact angle hysteresis, wetting of textured solids. 18.357 Interfacial Phenom., 2010, p. 59–64.
[41] McHale G, Shirtcliffe NJ, Newton MI. Contact-angle hysteresis on super-hydrophobic surfaces. Langmuir 2004;20:10146–9. https://doi.org/10.1021/la0486584.
[42] Bormashenko E. Progress in understanding wetting transitions on rough surfaces. Adv Colloid Interface Sci 2015;222:92–103. https://doi.org/10.1016/j.cis.2014.02.009.
[43] Kung CH, Sow PK, Zahiri B, Mérida W. Assessment and interpretation of surface wettability based on sessile droplet contact angle measurement: challenges and opportunities. Adv Mater Interfaces 2019;6. https://doi.org/10.1002/admi.201900839.
[44] Borodich FM. Fractal nature of surfaces. Encycl Tribol 2013:1264–9. https://doi.org/10.1007/978-0-387-92897-5_329.
[45] Liu X, Wang W, Pan A, Mei X, Liu B, Wang H. Robust superhydrophobic surface with romanesco broccoli-inspired fractal multilevel structures. Surf Interfaces 2025;58. https://doi.org/10.1016/j.surfin.2025.105877.
[46] Brown CA. Fractal-Related multiscale geometric characterisation of topographies. Character Area Surf Texture 2024:151–80. https://doi.org/10.1007/978-3-031-59310-9_6.
[47] Brown CA, Johnsen WA, Butland RM, Bryan J. Scale-Sensitive fractal analysis of turned surfaces. CIRP Ann Manuf Technol 1996;45:515–8. https://doi.org/10.1016/S0007-8506(07)63114-X.
[48] Brown CA, Childs BE, Bergstrom TS. Experimental methods using scale-sensitive, geometric analysis of surface textures for tribology. Proc STLE/ASME Int Jt Tribol Conf IJTC 2006 2006:2006. https://doi.org/10.1115/ijtc2006-12233.
[49] Brown CA, Blateyron F, Berglund J, Murrison AJ, Jeswiet JJ. Spatial frequency decomposition with bandpass filters for multiscale analyses and functional correlations. Surf Topogr Metrol Prop 2024;12. https://doi.org/10.1088/2051-672X/ad6f2f.
[50] Stemp WJ, Chung S. Discrimination of surface wear on obsidian tools using LSCM and RelA: pilot study results (area-scale analysis of obsidian tool surfaces). Scanning 2011;33:279–93. https://doi.org/10.1002/sca.20250.
[51] Stemp WJ, Lerner HJ, Kristant EH. Quantifying microwear on experimental mistassini quartzite scrapers: preliminary results of exploratory research using LSCM and scale-sensitive fractal analysis. Scanning 2013;35:28–39. https://doi.org/10.1002/sca.21032.
[52] James Stemp W, Childs BE, Vionnet S. Laser profilometry and length-scale analysis of stone tools: second series experiment results. Scanning 2010;32:233–43. https://doi.org/10.1002/sca.20200.
[53] Peta K, Stemp WJ, Stocking T, Chen R, Love G, Gleason MA, et al. Multiscale geometric characterization and discrimination of dermatoglyphs (Fingerprints) on hardened Clay—A novel archaeological application of the GelSight max. Mater (Basel) 2025;18:2939. https://doi.org/10.3390/ma18132939.
[54] Calandra I, Schulz E, Pinnow M, Krohn S, Kaiser TM. Teasing apart the contributions of hard dietary items on 3D dental microtextures in primates. J Hum Evol 2012;63:85–98. https://doi.org/10.1016/j.jhevol.2012.05.001.
[55] Cantor GJ, Brown CA. Scale-based correlations of relative areas with fracture of chocolate. Wear 2009;266:609–12. https://doi.org/10.1016/j.wear.2008.04.069.
[56] Ye XM, Zhang NK, Cheng R, Li CX. Effect of contact angle hysteresis on evaporation dynamics of a sessile drop on a heated surface. J Appl Fluid Mech 2022;15:1361–76. https://doi.org/10.47176/jafm.15.05.1069.
[57] Da Silva de Sa J, Ma W, Owen J, Hua Y, Neville A, Ponciano Gomes JAC, et al. Effect of flow rate on the corrosion behavior of API 5L X80 steel in Water-Saturated supercritical CO2 environments. Corrosion 2022;78:58–67. https://doi.org/10.5006/3939.
[58] Cirello A, Cucinotta F, Ingrassia T, Nigrelli V, Sfravara F. Fluid–structure interaction of downwind sails: a new computational method. J Mar Sci Technol 2019;24:86–97. https://doi.org/10.1007/s00773-018-0533-7.
[59] Wu S, Ma M. A contact angle hysteresis model based on the fractal structure of contact line. J Colloid Interface Sci 2017;505:995–1000. https://doi.org/10.1016/j.jcis.2017.06.078.
[60] Mortazavi V, D'Souza RM, Nosonovsky M. Study of contact angle hysteresis using the cellular potts model. Phys Chem Chem Phys 2013;15:2749–56. https://doi.org/10.1039/c2cp44039c.
[61] Peta K, Love G, Brown CA. Comparing repeatability and reproducibility of topographic measurement types directly using linear regression analyses of measured heights. Precis Eng 2024;536. https://doi.org/10.1016/j.precisioneng.2024.02.009.
[62] Gao Z, Zhang Y, Wei X, Peng L, Fu W, Wang W, et al. Evaluating the contact model for anisotropic non-Gaussian roughness in mixed lubrication regime. Phys Fluids 2023;35. https://doi.org/10.1063/5.0166240.
[63] Mohsen AAA, Song Y, Tang C, Huang Z. Dynamics of droplet impact on a rotating surface with different contact angles. Phys Fluids 2024;36. https://doi.org/10.1063/5.0241186.
[64] Lee JB, Derome D, Guyer R, Carmeliet J. Modeling the maximum spreading of liquid droplets impacting wetting and nonwetting surfaces. Langmuir 2016;32:1299–308. https://doi.org/10.1021/acs.langmuir.5b04557.
[65] Gao Z, Xi Y, Peng L, Fu W, Wang W, Hu W, et al. Normal and tangential contact models for mixed lubrication of mechanical interface. Phys Fluids 2022;34. https://doi.org/10.1063/5.0125283.
[66] Huai Y, Hu W, Song W, Zheng Y, Deng Z. Magnetic-field-responsive property of Fe3O4/polyaniline solvent-free nanofluid. Phys Fluids 2023;35. https://doi.org/10.1063/5.0130588.

[67] Xu M, Hu W, Han Z, Bai H, Deng Z, Zhang C. Symmetry-breaking dynamics of a flexible hub-beam system rotating around an eccentric axis. Mech Syst Signal Process 2025;222. https://doi.org/10.1016/j.ymssp.2024.111757.
[68] Hu W, Cui P, Han Z, Yan J, Zhang C, Deng Z. Coupling dynamic problem of a completely free weightless thick plate in geostationary orbit. Appl Math Model 2025;137. https://doi.org/10.1016/j.apm.2024.07.035.
[69] Hu W, Xi X, Song Z, Zhang C, Deng Z. Coupling dynamic behaviors of axially moving cracked cantilevered beam subjected to transverse harmonic load. Mech Syst Signal Process 2023;204. https://doi.org/10.1016/j.ymssp.2023.110757.